Iranian Journal of Physics Research, Vol. 25, No. 3, 2025
DOI: 10.47176/ijpr.25.3.72145

Temperature anisotropy in the magneto-inertial fusion process of $P^{11}B$ degenerate fuel

Fatemeh Khodadadi Azadboni*[1], Mohammad Mahdavi[2] and Elham Khademloo[2]
[1]Department of Physics Education, Farhangian University, P.O. Box 14665-889, Tehran, Iran
[2]Physics Department, University of Mazandaran, P. O. Box 47415-416, Babolsar, Iran

E-mail: f.khodadadi@cfu.ac.ir

(Received 24 July 2025 ; in final form 13 December 2025)

Abstract
This paper investigates the effect of temperature anisotropy on the reactivity and ignition of P-^{11}B degenerate fuel pellet in the Magneto-Inertial Fusion (MIF) process. Energy balance equations are solved to analyze the impact of temperature anisotropy and degeneracy parameter variations on ignition dynamics. The results demonstrate that increasing the degeneracy parameter amplifies fusion power while reducing bremsstrahlung power. Temperature anisotropy below unity ($\beta < 1$) enhances system stability, creating favorable conditions for ignition and achieving higher energy gain. During the pre-pulse phase, the system achieves its highest energy gain, and as time progresses, the gain gradually decreases. An increase in temperature anisotropy leads to the maximum energy gain occurring at a later time. The findings contribute to addressing the challenges associated with P-^{11}B fusion and improving the prospects of achieving efficient fusion reactions in magneto-inertial fusion.

Keywords: Magneto-Inertial Fusion, Degeneracy, P-^{11}B Fuel, Temperature Anisotropy

1. Introduction

Magnetized Inertial Fusion (MIF) combines the principles of Magnetized Inertial Confinement Fusion (ICF) and Magnetized Confinement Fusion (MCF) [1,2]. MIF presents a more comprehensive approach compared to traditional ICF and MCF, utilizing high-density plasma in the presence of powerful magnetic fields. This method requires less drive energy to ignite and heat the plasma [3, 4]. The concept of magneto-inertial fusion involves embedding magnetic flux in the fuel plasma, which is contained by a conductive shell acting as a magnetic flux shield. Both magnetic fields and laser driver energy are employed simultaneously to compress the fuel. At the critical density surface, the ponderomotive force generates electron beams, which are associated with the intense magnetic fields and expelled from the fusion fuel. As a result, the fuel plasma exerts high pressure on the surrounding material, triggering the formation of an intense shock wave and anisotropic temperature distribution within the fuel pellet's interior. In addition, heating techniques of cyclotron radiation deposit heat anisotropically, electron and ion cyclotron resonance heating both heats in the direction perpendicular to the magnetic field, whereas neutral beam heating preferentially heats in the direction of the beam [5]. Consequently, fuel plasmas in magneto-inertial fusion exhibit strong temperature anisotropy.

The presence of anisotropic distribution functions in velocity space can give rise to unstable modes that generate significant magnetic fields from the free energy of plasma particles. Anisotropy in temperatures parallel and perpendicular to the magnetic field can also drive instabilities [6,7]. Instability occurs when the perpendicular temperature of electrons exceeds the parallel temperature, or when the parallel temperature exceeds the perpendicular temperature. These instabilities and temperature anisotropy can affect the energy deposition of beams in the fuel plasma and the conditions required for ignition. It should be noted that temperature non-uniformity is inherent to magnetized plasma [8].

The fusion reaction between protons and Boron-11, historically discovered by Cockroft and Walton in 1932[9], revealed a significant anomaly in nuclear fusion reactions by operating at much lower energy levels than previously known in nuclear physics. Their pioneering work involved developing an accelerator to test whether the energy required for nuclei to produce reactions could be significantly lower than the MeV range [10]. Their groundbreaking discovery that only 150 keV were sufficient for protons to react with boron nuclei signified a major breakthrough in the field. Despite the greater difficulty of the P-^{11}B reaction compared to the D-T reaction, the interest in energy production was substantial due to the lower radioactivity produced per

unit of energy, as a result of only secondary reactions of the alpha particles with boron [11, 12]. The boron-proton reaction, which does not produce neutrons, is considered one of the most promising fusion reactions. With abundant isotopes, there is no need for artificial fuel production. This contrasted with the higher radioactivity generated from burning coal, attributable to the 2 ppm uranium content in all coal.

The challenge for laser-driven fusion using radially irradiated fuel pellets of P-^{11}B lies in the requirement for very high ignition temperatures and extremely high compression [13]. The goal of using the MIF method is to minimize factors that hinder confinement, thereby achieving sufficient plasma stability for net energy gain. Degeneracy is another significant factor that influences ignition efficiency. Lower ignition temperatures and reduced bremsstrahlung power compared to the classical state contribute to improved ignition conditions [14]. Controlling neutrons in plasma presents challenges due to their lack of charge, making it difficult to manipulate them with magnetic or electric fields.

Investigating these factors provides insights into the behaviour and performance of proton-boron degenerate fuel, facilitating advancements in fusion research and energy production [15, 16]. Continued efforts in these directions contribute to the advancement of fusion technology as a clean and sustainable energy source. Proton-boron fusion has been investigated theoretically [17-19], in laser-produced plasmas [20, 21], and via beam-target interactions in particle accelerators [22, 23]. Although ignition conditions for p-^{11}B fuel in magneto-inertial fusion have been examined in prior works [18-26], and [27] has specifically addressed these conditions assuming isotropic electron temperatures, the influence of temperature anisotropy on degenerate P-^{11}B fuel remains unexplored. The present study therefore introduces temperature anisotropy characterized by the parameter $\beta = T_{\perp}/T_{\parallel}$ as a key variable in the magneto-inertial fusion of degenerate fuel. This work aims to evaluate the impact of temperature anisotropy on ignition thresholds and energy gain in degenerate p-^{11}B systems within the magneto-inertial fusion framework.

2- Theoretical model

The proton-boron (P-^{11}B) reaction is indeed significant in the context of fusion research. It has several advantages over other fusion reactions, such as the deuterium-tritium (D-T) reaction. The P-^{11}B reaction involves a proton colliding with an ion of boron-11, resulting in the production of three alpha particles (helium nuclei) and the release of energy. The reaction can be represented as $p + 11B \rightarrow 3\alpha + 8.6$ MeV. Unlike reactions involving deuterium or tritium, the p-11B reaction does not require any radioactive isotopes as fuel. This eliminates concerns related to the handling, storage, and disposal of radioactive materials. The reaction only releases charged particles (alpha particles) rather than neutrons. Neutrons are uncharged particles that are difficult to contain and control. By avoiding neutron production, the P-^{11}B reaction mitigates certain engineering challenges associated with neutron radiation damage and the need for elaborate shielding. The P-^{11}B reaction has a higher energy gain compared to the D-T reaction. The energy gain is a measure of how much more energy is produced by the fusion reaction compared to the energy supplied to initiate and sustain the reaction. The P-^{11}B reaction offers the potential for higher energy gains, which is desirable for practical fusion power generation. However, it's important to note that the P-^{11}B reaction has its own challenges. The reaction cross-section (likelihood of the reaction occurring) is lower than that of the D-T reaction, primarily due to the greater electrostatic repulsion between the proton and the boron nucleus. Because Z = 5 for boron, the electrostatic repulsion of the reactants is five times as great as for the D-T reaction. Achieving the required reaction rates at practical temperatures and densities remains a significant scientific and engineering challenge.

2-1 State of fuel plasma in magneto-inertial fusion

Degeneracy conditions play a critical role in plasma by reducing ion-electron collisions, which has a direct impact on the ignition temperature. The degenerate state of fusion fuel, as mentioned earlier, offers advantages over the classical state by minimizing losses from bremsstrahlung radiation and improving fuel ignition. The electron anisotropy degree is denoted by $\Theta = k_B T_e/\varepsilon_f$, where k_B represents the Boltzmann constant, T_e is the electron temperature in kilo-electron volts, and ε_f is the Fermi energy, which corresponds to the highest filled energy level and obtained from the following relationship [28]

$$\varepsilon_f = \frac{1}{8}\frac{h^3}{m_e}\left(\frac{3n_e}{\pi}\right)^{2/3} = 2.19\times10^{-15} n_e^{2/3}[eV] \quad (1)$$

Here, $\hbar$ denotes the reduced Planck's constant, m_e represents the electron mass, and n_e represents the electron number density. When Θ is less than 0.1, electrons are in a state of complete degeneracy, and thermal effects become negligible. Therefore, the primary requirement for maintaining degenerate conditions is to ensure that the electron temperature remains lower than the Fermi temperature throughout the burning process. In the range where $0.1 < \Theta < 1$, electrons exist in a partially degenerate state where both thermal and quantum effects coexist. Conversely, when Θ exceeds 1, electrons are in a non-degenerate and classical state, and quantum effects become insignificant except during short-term collisions.

In the low-temperature range where the fuel is partially degenerate, the degenerate gas exhibits high resistance to compression due to the Pauli exclusion principle. Electrons are unable to transition to lower-energy states that were previously occupied, resulting in an increase in the degenerate pressure. This increase in pressure, known as the degenerate pressure, can be expressed as [28]

$$p_{\deg} = \frac{2}{5} n_e \varepsilon_f \quad (2)$$

The degenerate pressure plays a crucial role in maintaining the degeneracy of the plasma and contributes to the overall behavior of the system.

The degeneracy parameter $\alpha = \mu / k_B T_e$ remains constant during adiabatic compression and measures the fuel's entropy, which is why it is often referred to as the adiabatic parameter. In the case of a degenerate partially electron fluid, the chemical potential μ has a positive value. Adding a particle to the system at constant entropy and volume requires an increment in internal energy. This positive chemical potential indicates that in a degenerate state, the system's energy increases when a new particle is added at the Fermi energy, even at zero entropy. In contrast, for a classical system, the chemical potential μ is negative. In this case, a new particle can be added with zero energy, but to maintain entropy, the system's internal energy must decrease. However, in a degenerate system, the degeneracy parameter α equals the Fermi energy (ε_f), denoting the chemical potential. Therefore, in a degenerate system, $\alpha = \varepsilon_f / (k_B T_e)$. The appropriate formula for the degeneracy parameter can be expressed as [29]

$$\alpha = -\frac{3}{2}\ln\Theta + \ln\frac{4}{3\sqrt{\pi}} + \frac{A\Theta^{-(b+1)} + B\Theta^{-(b+1)/2}}{1 + A\Theta^{-b}} \qquad (3)$$

where, A=0.25054, B=0.072 and b=0.858. This equation captures the relationship between the degeneracy parameter, the Fermi energy, and the electron temperature (T_e), providing insights into the degenerate behavior of the p-11B fuel system. In magneto-inertial fusion (MIF), plasmas are commonly enveloped by a magnetic field. To analyze the behavior of the plasma in this context, a parameter called ϵ is introduced. The parameter ϵ is defined as

$$\epsilon = \frac{P}{B^2/2\mu_0}, \qquad (4)$$

representing the ratio of plasma kinetic pressure to magnetic pressure, $B^2/2\mu_0$ [30], where, p is $p = n_i k_B T_i + n_e k_B T_e$ and B is the magnetic field and μ_0 is the vacuum magnetic permeability. This parameter ϵ serves as an indicator of the relative strengths of the plasma pressure and the magnetic pressure. In magneto-inertial fusion, $\epsilon \approx 1$ is assumed to ensure dynamic equilibrium between thermal expansion and magnetic compression forces.

To further characterize the system, we can define the Fermi energy in terms of the magnetic field and the degeneracy parameter using the following equations,

$$\varepsilon_f = \frac{5B^2}{4\alpha\mu_0 n_e}. \qquad (5)$$

When a high-power laser pulse >10^{21} W/cm^2 interacts with the P-11B fuel, the plasma of the fuel will be heated predominantly in the velocity dimension along the wave propagation direction, resulting in a temperature anisotropy of the electron distribution. This leads to the generation of a shock wave by the laser beam in the fuel, resulting in different ion and electron temperatures.

In the presence of temperature anisotropy and anisotropic plasma conditions, turbulence is induced to promote equilibration and reduce the free energy associated with the anisotropy. This turbulence introduces oscillations in the plasma, which can have implications for confinement and energy transfer mechanisms. Furthermore, the presence of a strong magnetic field in the target plasma poses challenges to heat transfer during compression. However, this magnetic field plays a facilitative role in providing the necessary compression heat for the plasma to reach nuclear fusion temperatures. Consequently, the strong magnetic field enhances the deposition of energy from alpha particles into the fusion plasma.

To investigate the effect of temperature anisotropy on degenerate fuel, we introduce the temperature anisotropy parameter β, defined as the ratio of the perpendicular temperature ($T_\perp$) to the parallel temperature ($T_\parallel$). In this scenario, the electron temperature can be expressed as a function of the anisotropy parameter $T_e = \beta^{\frac{2}{3}} T_\parallel$. Additionally, the perpendicular and parallel effective temperatures with respect to wave propagation are defined as follows [31]

$$T_\perp = \frac{m_e}{2n_0}\int v_z^2 \, f_0(v) d^3v \ , \qquad (6)$$

$$T_\parallel = \frac{m_e}{n_0}\int v_x^2 f_0(v) d^3v \quad . \qquad (7)$$

where, f_0 is the anisotropy distribution function.

2-2 Ignition conditions for magneto-inertial fusion

In Magneto-Inertial Fusion (MIF), the conditions for ignition are similar to those in other fusion concepts, such as magnetic confinement fusion and inertial confinement fusion. The primary condition for ignition in MIF is achieving a self-sustaining burn, where the energy produced by fusion reactions is sufficient to sustain the fusion process. The conditions for ignition in MIF involve the production of power through the fusion process that exceeds the power losses. The power is generated through the fusion of ions. The products resulting from the fusion process inject a fraction of the energy produced by fusion back into the fuel, and a fraction of this energy is lost. Therefore, for ignition to occur, the fusion power density must exceed the total loss power density throughout the burn phase. The power generated by fusion, including the energy injected back into the fuel, must exceed the power losses from the system

$$W_f - W_B - W_{me} - W_{mi} - W_{he} - W_{cyc} \geq 0 \ , \qquad (8)$$

where W_f , W_B, W_{he}, W_{me}, W_{mi}, W_{cy} indicates the deposited power density by α particles, the power density of bremsstrahlung radiation, the thermal conductivity of electrons, the mechanical work of electrons and ions in the degenerate state, the power of the cyclotron radiation respectively. It's important to note that achieving ignition in magnetically confined fusion is a significant challenge, and current fusion experiments and research are focused on reaching this goal. The alpha particles created in nuclear fusion reactions bring about the fusion power density, the equation of which is written as follows in magnetically confined fusion [32]

$$W_f\left[\frac{erg}{cm^3.s}\right] = f_\alpha n_p n_B < \sigma v >_{p11B} E_\alpha = \left(\frac{\epsilon B}{2\mu_0}\right)^2 \frac{<\sigma v>_{p11B} E_\alpha}{T_e^2(z_1+z_2+2)} \left(\frac{\epsilon B}{2\mu_0}\right)^2 = \frac{<\sigma v>_{p11B} E_\alpha}{(\beta^{2/3} T_\parallel)(\frac{\varepsilon_f}{k_B \alpha})(z_1+z_2+2)}, \quad (9)$$

where T is temperature in kilo-electron volts, E_α is the energy released from fusion, z_1, z_2 the atomic number of each particle. The ratio of plasma pressure to magnetic pressure, ϵ, is assumed to be approximately 1 in this case. In addition, $< \sigma v >_{p11B}$ is average rate of reactivity for the (p-^{11}B) reaction which is obtained from the following relationship [32]

$$< \sigma v >_{p11B} \left(\frac{cm^3}{s}\right) = 5.41 \times 10^{-15} T_i^{-3/2} \exp\left(\frac{-148}{T_i}\right) + 6382 \times 10^{-16} \zeta^{-5/6} \left(\frac{17.708}{T_i^{1/3}}\right)^2 \exp\left(-3\zeta^{1/3} \frac{17.708}{T_i^{1/3}}\right), \quad (10)$$

where, $\zeta = -\frac{-59.357\times10^{-3}T_i + 1.0404\times10^{-3}T_i^2 - .0091653\times10^{-3}T_i^3}{1+210.65\times10^{-3}T_i + 2.7621\times10^{-3}T_i^2 + .00098305\times10^{-3}T_i^3}$.

One of the most important energy loss mechanisms is bremsstrahlung radiation, where an electron, under the influence of the force from close collisions with heavy atoms, is deflected from its original path and accelerated. The accelerated electron emits electromagnetic energy radiation, which according to quantum theory includes discrete quanta (photons). Through photon emission, the kinetic energy of the electron decreases, leading to a decrease in plasma temperature. Results have shown that bremsstrahlung energy loss in degenerate plasma is much less than in the classical case. The bremsstrahlung power equation is derived from the following relationship [33]

$$W_B\left[\frac{W}{m^3}\right] = \frac{KT_e^2}{h}\left[F_1(\xi) - \frac{1}{2}\ln^2(e^\xi + 1)\right], \quad (11)$$

where,

$$K = \left(\frac{256\pi^3}{3\sqrt{3}}\right)\left(\frac{1}{4\pi\varepsilon_0}\right)^3 \frac{Z^2 e^6 n_i}{h^3 c^3}, \qquad \xi = \frac{\epsilon_f}{T_e}.$$

The Dirac delta function integrals based on the approximation $\xi \geq 1$ (degenerete state) are defined as follows

$$F_{1/2}(\xi) = \lim \int_{\xi\geq1} \frac{x^{1/2}dx}{\exp(x-\xi)+1} = \frac{2}{3}\xi^{2/3}, \quad (12)$$

$$F_1(\xi) = \lim \int_{\xi\geq1} \frac{xdx}{\exp(x-\xi)+1} = \frac{1}{2}\xi^2 + \frac{\pi^2}{6}. \quad (13)$$

The ratio of radiation emission in degenerate plasma to the classical state can be written as

$$\frac{W_{deg}}{W_{class}} = \frac{\sqrt{\pi}}{2}\frac{1}{F_{1/2}(\xi)}[F_1(\xi) - \frac{1}{2}\ln^2(e^\xi + 1)]. \quad (14)$$

Based on the above relationships, the recent equation can be written as

$$\frac{W_{deg}}{W_{class}} = \frac{\pi^2\sqrt{\pi}}{8}\left(\frac{\beta^{\frac{2}{3}} T_\parallel}{\varepsilon_f}\right). \quad (15)$$

The electric current per unit area from the hot spot causes energy loss from the fuel disk surface in the form of heat, which is obtained from the following relationship [34]

$$W_{he}[\frac{erg}{cm^3.s}] = 3A_e \frac{T_e^{7/2}(1/1+3.3Z_i))}{R^2 Z_i \log\Lambda}, \quad (16)$$

where, $A_e = \frac{5.529\times10^{28}}{(1.6022\times10^{-9})^{2.5}}(erg^{-5/2}cm^{-1}s^{-1})$.

For $T_\parallel \neq T_\perp$, the thermal conductivity of electrons is defined by

$$W_{he}[\frac{erg}{cm^3.s}] = 3A_e \frac{(\beta^{2/3}T_\parallel)^{7/2}(1/1+3.3Z_i))}{R^2 Z_i \log\Lambda}, \quad (17)$$

The Coulomb logarithm in degenerate plasma is defined as follows

$$\log\Lambda \cong \log[0.1718(n_e)^{-1/3}\rho_c], \quad (18)$$

where, $\rho_c = \frac{Z_i Z_j e^2}{2E_\alpha}$. Here i, j represents the ion species. When the fuel disk starts to burn, the pressure generated in the fusion reactions expands the fuel disk. As a result, this expansion reduces the density and the rate of fusion reactions, meaning that some of the plasma energy is wasted by mechanical expansion. The power density of the mechanical work of electrons and ions on the hot spot environment is obtained from the following relationship

$$W_{me} = \frac{4\pi C_s R^2 n_e k_B (\beta^{2/3} T_\parallel)}{V}, \quad (18)$$

$$W_{mi} = \frac{4\pi C_s R^2 n_i k_B T_i}{V}. \quad (19)$$

Here $C_s = \sqrt{\gamma P/\rho}$ is the sound speed, and γ=5/3and P is the plasma pressure. In a high-temperature plasma, energy loss occurs not only in the form of bremsstrahlung radiation but also in a different way through nuclear reactions. Considering the confinement of the plasma at very high temperatures based on the use of a magnetic field, ions and electrons oscillate at specific frequencies known as gyrofrequency or cyclotron frequency. The power density of cyclotron radiation per unit volume can be derived from the following relationship, assuming the electrons have a Maxwellian distribution

$$W_{cyc} = \frac{4e^4 k_B}{3m_e^3 c^5} B^2 n_e (\beta^{2/3} T_\parallel), \quad (20)$$

where c is the speed of light.The emission of cyclotron radiation is an important energy loss mechanism in high-temperature plasmas, and its impact on the overall energy balance needs to be considered when studying and analyzing plasma behavior in the presence of strong magnetic fields. The necessary condition for magnetic confinement is that the kinetic pressure of plasma particles be smaller than the magnetic pressure, meaning

$$(n_i + n_e)k_B T \leq \frac{B^2}{2\mu_0} \quad (21)$$

This implies that confinement requires an imposed magnetic pressure that dominates over the intrinsic kinetic pressure of the particles. In the case of magneto-inertial fusion, it is considered that the ratio of plasma pressure to magnetic pressure is approximately equal to one ($\epsilon \approx 1$) and

$$\frac{B^2}{8\pi} = n_i k_B T_i + n_e k_B \left(\frac{\varepsilon_f}{\alpha k_B}\right). \quad (22)$$

This assumption implies that the plasma pressure is roughly of the same order as the magnetic pressure, indicating a balance between the two. This balance is significant for the behavior of the plasma in the magneto-inertial fusion process. By substituting equation (22) into equation (20), the power density of cyclotron radiation can be obtained as

$$W_{cyc}[\frac{KeV}{cm^3.s}]=\frac{32\pi e^4 {k_B}^2}{3{m_e}^3 c^5}(n_i T_i+n_e(\frac{\varepsilon_f}{\alpha k_B}))n_e(\beta^{2/3}T_{\|}).(23)$$

2-3Energy balance equations

Shock waves are created by laser beams in the target, with different temperatures for ions and electrons. Therefore, we must consider the changes in the temperatures of ions and electrons. Ions and electrons in the plasma are mainly at different temperatures for two reasons. First: Bremsstrahlung radiation by electrons, Second: High-temperature fusion plasma by ions. As a result, the ion temperature must be higher than the electron temperature. Therefore, in ion-electron collisions, we expect energy transfer from ions to electrons. Therefore, energy balance equations dependent on ions and electrons are written as follows [35]

$$\frac{3}{2}\frac{\partial}{\partial t}(n_e k_B(\beta^{2/3}T_{\|}))=\eta_d W_d+\eta_\alpha W_f+W_{ie}-W_B-W_{me}-W_{he}-W_{cyc} \quad (24)$$

$$\frac{3}{2}\frac{\partial}{\partial t}(n_i k_B T_i)=(1-\eta_d)W_d+(1-\eta_\alpha)W_f-W_{ie}-W_{mi}. \quad (25)$$

The driver power density, W_d, induced by the laser-piston can be calculated using equation [32]

$$W_d=\frac{p_d}{4\pi\frac{R^3}{3}} \quad (26)$$

where, P_d, is the power of the proton-driver beam, given by equation

$$p_d=\frac{8}{3\sqrt{\pi}}\frac{E_{tot}}{\tau}(\frac{\tau}{t})^6\exp[-(\frac{\tau}{t})^2]. \quad (27)$$

In equation (27), τ represents the pulse duration, which is given by $\tau=\sqrt{(m_p)d^2/(2T_p)}$, where d is the target-to-spot distance, and E_{tot} is the total energy. Also, η_d the fraction of drive energy deposited by electrons, (1- η_d) the fraction of drive energy deposited by ions, η_α the alpha particle energy fraction resulting from fusion deposited by electrons and (1- η_α) the alpha particle energy fraction resulting from fusion deposited by ions. The symbol W_{ei} is the ion-electron energy exchange power density is in the degenerate state and can be calculated from the following equation [32]

$$W_{ie}=\frac{3}{2}n_i T_i \nu_{ie}(T_e). \quad (28)$$

The collision frequency between ions and electrons in degenerate plasma, ν_{ei}, is expressed as follows [14]

$$\nu_{ei}=3.47\times10^{13}(Z^2/\mu_i)s^{-1}, \quad (29)$$

where, μ_i is the nucleus mass in the unit of the proton mass.

2-4 Energy gain in degenerate plasma of p11B fuel

The important point considered in nuclear fusion reactions is to have a relatively high reaction rate in a small volume and to have a comparable energy output compared to other methods of energy production. A critical quantity in any energy production system, such as nuclear fusion systems, is energy efficiency. In the process of nuclear fusion, if the energy transferred from the fusion products is greater than the input energy to the system, it is considered positive efficiency. Therefore, energy efficiency is defined as follows

$$Gain=\frac{E_{fusion}}{E_{input}}. \quad (30)$$

Efficiency is a measure of how effectively the input energy is converted into usable output energy in the fusion process. The goal in nuclear fusion research is to achieve a high energy output with a minimal input energy requirement, thus maximizing the energy efficiency of the system. The energy efficiency equation used here is defined as follows[28]

$$G=\frac{4\pi}{3}\frac{q_{PB}}{E_d}\left[\rho_h {R_h}^3+({R_f}^3-{R_h}^3)\rho_c\right]\frac{H_h+H_c}{H_B+H_h+H_c}, \quad (31)$$

where, q_{PB}, E_d , ρ_h and R_h are respectively the fusion energy released per unit of fuel mass, start-up energy, hot spot density, and hot spot radius. The parameter η in the direct driver targets is considered to absorb the driver energy and couple it to the fuel, which here is assumed to be equal to 0.1. Here, $R_f=\sqrt{\eta E_d/2\pi p}$, $H_c=\rho_c(R_f-R_h), H_h=\rho_h R_h$, $H_B=8C_s m_f/<\sigma v>$ and $\rho_c=(\alpha A_{\deg})^{\frac{-3}{5}}p^{\frac{3}{5}}$ the degenerate constant, A_{deg} , is defined by

$$A_{\deg}=\frac{2}{5}\frac{\hbar}{2m_e}\frac{(3\pi^2)^{\frac{2}{3}}}{[\frac{m_P+m_B}{2}]^{\frac{5}{3}}}. \quad (32)$$

Here m_B, m_p, m_e, and m_f are respectively the masses of boron, proton, and electron and the average mass of fuel ions.

2-5 Numerical solution procedure

The energy balance equations (24) and (25), together with the auxiliary relations for fusion reactivity ⟨σv⟩, bremsstrahlung emission, cyclotron radiation, and degeneracy effects, are solved numerically using a fourth-order Runge–Kutta (RK4) scheme with adaptive time stepping. The system is reduced to a set of two ordinary differential equations for the electron temperature $T_e(t)$ and ion temperature $T_i(t)$, assuming quasi-neutrality and instantaneous pressure balance. The driver power is modeled as a Gaussian pulse (Eq. 27) with FWHM ≈ 100 ns, consistent with pulsed-power driver characteristics. All loss and gain terms are updated at each time step. The numerical integration is performed until the burn fraction exceeds 30% or the temperature begins to decline. Convergence tests with time steps of 10^{-15}–10^{-16} s confirm that relative errors in energy gain remain below 0.5 %.

3- Results and discussions

Achieving and developing fusion conditions in a laboratory setting with the aim of cost reduction directs attention towards the method of magnetically confined fusion. In this context, energy balance equations have been solved considering initial conditions of $\varepsilon = n_B / n_p = 0.33$, $R = 10^{-4}$ cm, and $\rho = 10^4$ g/cm^3 for proton-boron degenerate fuel.

Initially, the power density from fusion, loss powers, and ultimately energy efficiency are examined. Boron-11 fuel is not viable at magnetic field strengths below 10^6G. At magnetic fields less than 10^6 G, fusion does not occur because the fusion power is lower than the loss power. Magnetic fields in the megatesla range are not achievable with conventional Z-pinch techniques (≤ 100 T). However, in Magneto-Inertial Fusion (MIF), particularly in MagLIF configurations, initial fields of 10–30 T are generated using external solenoids and are amplified to 10^3–10^4 T during dynamic compression. Slutz et al. show that the magnetic field is approximately proportional to the inverse square of the fuel radius and can exceed 100 MG (equivalent to > 10,000 T) during compression [30].

Additionally, it has been demonstrated that increasing the magnetic field strength leads to a rise in the maximum fusion power of the fuel. Furthermore, as the degenerate parameter increases, the maximum fusion power of the fuel also rises due to the reduction in loss powers. The use of higher magnetic fields in our study was motivated by the exploration of extreme conditions that could potentially enhance fusion power for P-^{11}B degenerate fuel. We believe that investigating these scenarios can provide valuable insights into the upper limits of the Magneto-Inertial Fusion process. This will provide a balanced perspective on how varying magnetic field strengths can affect the outcomes of P-^{11}B fusion. The impact of different temperature anisotropies, represented by beta values greater and less than one, are being examined.

Figure 1 illustrates the power density from fusion over the time interval (0-10^{-12} s). The calculations consider degeneracy parameters $\alpha = 1$ and $\alpha = 1.5$. From the figures, it is evident that an increase in temperature anisotropy leads to a decrease in the power density from fusion. However, the power density from fusion increases with time, indicating a cumulative effect.

For $\beta = 0.25$, $B = 10^7$ G, α=1, at time 10^{-12}s, the power density from fusion is 3.02×10^{39} erg/s.cm^3. With the same temperature anisotropy and magnetic field values, but with $\alpha = 1.5$, the power density from fusion increases to 4.5×10^{39} erg/s.cm^3. It is evident that as the degeneracy parameter increases, the power density from fusion also increases. For $\beta = 0.5$, β =10, β =100, and α=1, the power density from fusion is 1.9×10^{39} erg/s.cm^3, 3.87×10^{38} erg/s.cm^3 and 8.33×10^{37} erg/s.cm^3 respectively. Hence, it can be concluded that for $\beta \leq 1$, the power density from fusion is on the order of 10^{39} erg/s.cm^3. However, for $\beta > 1$, a tenfold increase in the temperature anisotropy leads to a roughly tenfold decrease in the power density from fusion.

Figure 2 illustrates the power density from bremsstrahlung radiation for different temperature anisotropies with degeneracy parameters $\alpha = 1$ and $\alpha = 1.5$ over the time interval (0-10^{-12} s). The figures demonstrate that the power density from bremsstrahlung radiation exhibits an increase with higher temperature anisotropy parameters, as well as with the progression of time. For β=0.25, α=1, at time 10^{-12}s, the power density from bremsstrahlung radiation is 6×10^{32} erg/s.cm^3. When $\alpha = 1.5$ with the same magnetic field, the power density from bremsstrahlung radiation decreases to 5.93×10^{32} erg/s.cm^3. Hence, it can be concluded that with an increase in the turbulence parameter, the power density from bremsstrahlung radiation decreases.

Figure 3 illustrates the power density from cyclotron radiation over the time interval (0-10^{-12} s), considering temperature anisotropies greater and less than one and degeneracy parameters $\alpha = 1$ and $\alpha = 1.5$. The figure clearly demonstrates that the power density from cyclotron radiation exhibits an increase with higher temperature anisotropy values, as well as with the progression of time. Furthermore, the effects of the degeneracy parameter and magnetic field on cyclotron radiation are explored for temperature anisotropies both less than and greater than one.

For β=0.25, α=1, at time 10^{-12}s, the power density from cyclotron radiation is 1.9×10^{35}erg/s.cm^3. For the same field but with $\alpha = 1.5$, the power density from cyclotron radiation decreases to 1.8×10^{35} erg/s.cm^3. Therefore, it can be observed that with an increase in the degeneracy parameter, the power density from cyclotron radiation decreases.

Now, let's examine the results for temperature anisotropy greater than one. For instance, for $\beta = 10$ and $\alpha = 1$, the power density from cyclotron radiation is 2.2×10^{36} erg/s.cm^3. With the same temperature anisotropy and magnetic field but with $\alpha = 1.5$, the power density from cyclotron radiation becomes 2.1×10^{36} erg/s.cm^3. Consequently, it can be observed that with an increase in the degeneracy parameter, the power density from cyclotron radiation decreases.

For $\beta = 0.5$ and $\alpha = 1$, the power density from cyclotron radiation is 3.02×10^{35} erg/s.cm^3. However, for $\beta = 100$ with the same magnetic field and $\alpha = 1$, the power density from cyclotron radiation increases significantly to 1.03×10^{37} erg/s.cm^3. Therefore, it can be observed that if $\beta \leq 1$ for all fields and degeneracy parameters, the power density from cyclotron radiation is of the order of 10^{35} erg/s.cm^3. However, for $\beta > 1$, with a tenfold increase in temperature anisotropy, the power density from cyclotron radiation increases approximately in the same proportion, roughly tenfold.

Figure 4 depicts the energy efficiency over the time interval (0-10^{-12}s), considering temperature anisotropies greater and less than one. The turbulence parameters $\alpha = 1$ and $\alpha = 1.5$ are used, along with an efficiency η of 10%, a fuel mass m_f of 0.5 g, and an initial temperature T_i =200 keV. As evident from the figures, the energy efficiency decreases with an increase in temperature anisotropy. There is an initial peak in energy efficiency during the pre-pulse phase, followed by a gradual decrease over time. For $\alpha = 1$, and temperature

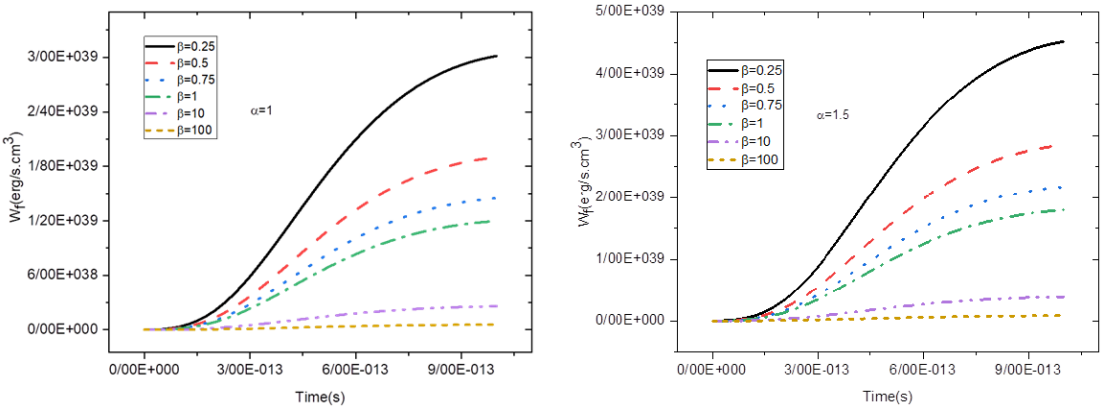

Figure 1. The fusion power versus time for different temperature anisotropy, degeneracy parameters, α=1, α=1.5.

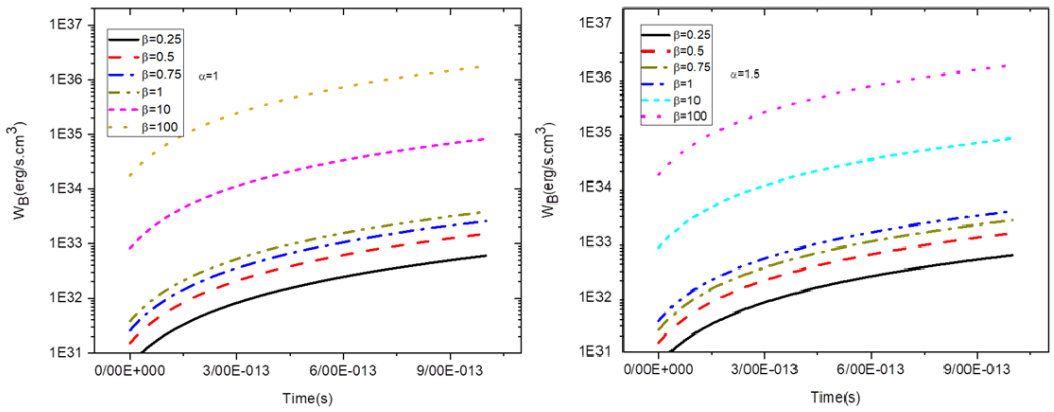

Figure 2. The bremsstrahlung power versus time for different temperature anisotropy, degeneracy parameters, α=1, α=1.5.

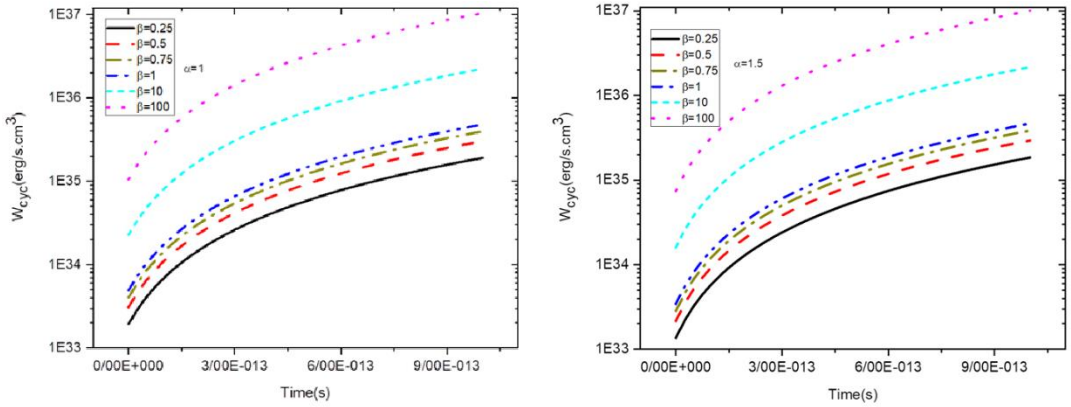

Figure 3. The cyclotron radiation power versus time for different temperature anisotropy, degeneracy parameters, α=1, α=1.5.

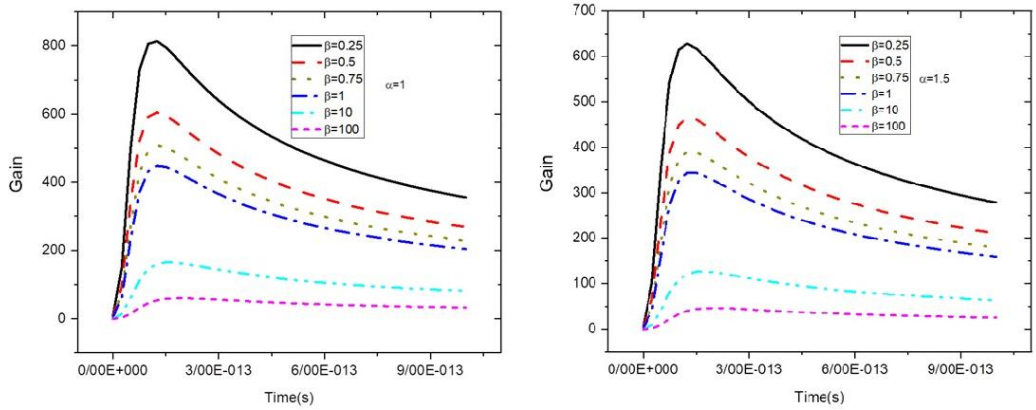

Figure 4. The energy gain versus time for different temperature anisotropy, degeneracy parameters, α=1, α=1.5, and T_i=200keV, η = 10%, m_f = 0.5 g.

anisotropies $\beta \leq 1$, the highest energy efficiency occurs at a time of 1.25×10^{-13} s. However, for $\beta = 10$ and $\beta = 100$, the highest energy efficiency occurs at times of 1.5×10^{-13} s and 2×10^{-13} s, respectively. Hence, it can be concluded that with an increase in temperature anisotropy, the maximum energy efficiency occurs at a later time.

4. Conclusion

In this paper, the effect of the temperature anisotropy on the P-^{11}B degenerate fuel ignition criterion in the magneto-inertial fusion process is investigated. In the process, the power density resulting from fusion, loss powers, and energy efficiency have examined. The results reveal that temperature anisotropy has a significant impact on these parameters. Increasing temperature anisotropy leads to a decrease in power density from fusion, while the density of loss powers such as bremsstrahlung and cyclotron radiation increases, resulting in decreased energy efficiency. However, when the temperature anisotropy is less than one ($\beta < 1$), the system becomes more stable, promoting better conditions for ignition and achieving higher energy efficiency. The energy efficiency of the system under consideration shows a decrease with an increase in temperature anisotropy. During the pre-pulse phase, the system attains its peak energy efficiency, which gradually decreases as time progresses. Additionally, an increase in temperature anisotropy causes the maximum energy efficiency to occur at a later time. Achieving $\beta < 1$ (i.e., $T_{\perp} < T_{\parallel}$) in magneto-inertial fusion (MIF) plasmas is challenging but feasible, requiring selective heating along the magnetic field direction to promote parallel temperature dominance. Parallel neutral beam injection (NBI) along the magnetic axis deposits energy primarily into the parallel ion temperature $T_{\parallel}$, as beam ions thermalize rapidly along field lines while perpendicular heating is suppressed by gyromotion [36]. This technique, adaptable to MagLIF via axial beam ports, enables selective $T_{\parallel}$ enhancement to achieve $\beta < 1$. Additionally, in adiabatic compression within cylindrical geometry, the perpendicular temperature scales as $T_{\perp} \propto R^{-4/3}$, while the parallel temperature remains nearly constant in the presence of a strong axial magnetic field [30]. This scaling arises from the conservation of the perpendicular adiabatic invariant and the R^{-2} density increase during implosion. Furthermore, ion cyclotron resonance heating (ICRH) with wave vectors aligned parallel to B ($k_{\parallel} >> k_{\perp}$) selectively increases $T_{\parallel}$ through resonant absorption at the ion cyclotron frequency. These techniques can be adapted to MIF targets with embedded axial fields to enhance stability and confinement.

Finding the optimal balance between system degeneracy, temperature anisotropy, and other factors becomes crucial for maximizing fusion power and energy efficiency. These findings have significant implications for the optimization of fusion processes and energy production. They underscore the need for further research and development in these areas to deepen our understanding and enhance the efficiency of fusion systems. By investigating these factors, we can gain valuable insights into the behavior and performance of degenerate proton-boron fuel. This knowledge can pave the way for advancements in fusion research and energy production. Continued efforts in these directions will contribute to the advancement of fusion technology and its potential as a clean and sustainable energy source.

5-Data availability

All data generated or analyzed during this study are included in this research paper.

References

1. G A Wurden, S C Hsu, T P Intrator, T C Grabowski, J H Degnan, M Domonkos, P J Turchi, E.M Campbell, D B Sinars, M C Herrmann, and R Betti, Journal of Fusion Energy **35** (2016) 69.
2. D H Barnak, J R Davies, R Betti, M.J Bonino, E M Campbell, V Y Glebov, D R Harding, J P Knauer, S P Regan, A B Sefkow, and A J Harvey-Thompson, Physics of Plasmas **24** (2017) 056310-1.
3. S C Hsu and J L Samuel, Journal of Fusion Energy **38** (2019) 182.
4. S A Slutz, and R A Vesey, Physical review letters **108** (2012) 025003.
5. M Kouhi, M Ghoranneviss, B Malekynia, H Hora, G H Miley, A H Sari, N Azizi, and S S Razavipour, Laser and Particle Beams **29** (2011) 125.
6. E J Kolmes, M.E Mlodik and N J Fisch, Physics of Plasmas **28** (2021) 052107.
7. S Amininasab, R Sadighi-Bonabi, and F.Khodadadi Azadboni, Contributions to Plasma Physics **59** (2019) e201800111.
8. T Pahuja, A Kumar, H Sagar, R Gupta, and J Sharma, AIP Advances **14** (2024) 025136.
9. J D Cockroft and E.T.S Walton, Proc. Roy. Soc. London A **137** (1932) 229.
10. N Azizi, H Hora, G H Miley, B Malekynia, M Ghoranneviss, and X He, Laser and Particle Beams **27** (2009) 201.
11. J H Nuckolls, "Laser-induced implosion and thermonuclear burn. In Laser Interaction and Related Plasma Pheonomena" (H Schwarz and H Hora, Eds.) (New York: Plenum Press,1974).
12. T Weaver, G Zimmerman, and LWood, "Exotic CTR fuels: Non-thermal effects and laser fusion applications" (Report UCRL-74938. Livermore, CA: Lawrence Livermore Laboratory,1973).
13. H Hora and G H Miley, International Conference on Nuclear Engineering **49347** (2010) 611-620.
14. S Son, and N J Fisch, Physics Letters A **329** (2004) 76.
15. S Eliezer, and J M Martinez-Val, Laser and Particle Beams **16** (1998) 581.
16. W McKenzie, D Batani, T A Mehlhorn, D Margarone, F Belloni, E M Campbell, S Woodruff, J Kirchhoff, A

Paterson, S Pikuz, and H Hora, Journal of Fusion Energy **42** (2023) 17.
17. F A Geserand M Valente, Radiat. Phys. Chem. **167** (2020) 108224.
18. P T León, S Eliezer, M Piera, and J M Martínez-Val, In Current Trends in International Fusion Research: Proceedings of the Fifth Symposium NRC Research Press, (2008) p.323.
19. W M Nevins and R Swain, Nucl. Fusion **40** (2000) 865.
20. D Margarone, J Bonvalet, L Giuffrida, A Morace, V Kantarelou, M Tosca, D Raffestin, P Nicolai, A Picciotto, Y Abe, et al. Appl. Scie. **12** (2022) 1444.
21. S Stave, M W Ahmed, R H France III, S S Henshaw, B Müller, B A Perdue, R M Prior, M C Spraker, and H R Weller, Phys. Lett. B **696** (2011) 26.
22. M Sikora, and H Weller, J. Fusion Energy **35** (2016) 538.
23. R M Magee, K Ogawa, T Tajima, I Allfrey, H Gota, P McCarroll, S Ohdachi, M Isobe, S Kamio, V Klumper, and H Nuga, Nature communications **14** (2023) 955.
24. F Khodadadi Azadboni, A Khademloo, and M Mahdavi, Iranian Journal of Physics Research **24** (2024) 99.
25. M Mahdavi and A Gholami, Indian Journal of Physics **96** (2022) 869.
26. F Khodadadi Azadboni, A Khademloo, and M Mahdavi, Iranian Journal of Physics Research **23** (2023) 147.
27. M Mahdavi, M Bakhtiyari, and A Najafi, Indian Journal of Physics **97** (2023) 1277.
28. S Atzeni, and J Meyer-ter-Vehn, The Physics of Inertial Fusion: BeamPlasma Interaction, Hydrodynamics, Hot Dense Matter, Oxford University Press (2004).
29. S Pfalzner, An Introduction to Inertial Confinement Fusion (CRC Press, 2006), Chap. 3.
30. S A Slutz et al., Phys. Plasmas **17** (2010) 056303.
31. S P Gary, Theory of space plasma microinstabilities (No. 7). Cambridge university press (1993).
32. S Eliezer, Z Henis, N Nissim, S V Pinhasi, and J M M Val, Laser and Particle Beams **33** (2015) 577.
33. M Mahdavi, A Gholami, and O N Ghodsi. Chinese Journal of Physics **68** (2020) 596.
34. MS Chu, Phys. Fluids **15** (1972) 413.
35. M Mahdavi, and A Gholami, Fusion Engineering and Design **142** (2019) 33.
36. W M Stacey, Fusion Plasma Physics, 2nd Edition, Wiley-VCH (2012).